Journal of Thermal Analysis and Calorimetry (2023) 148:1501–1510
https://doi.org/10.1007/s10973-022-11802-w

Effect of Cr^{3+} ions on the crystallization of calcium silicate hydrates ($CaO/SiO_2 = 1.5$) under hydrothermal conditions and their thermal stability

I. Gedeike[1] · K. Baltakys[1] · A. Eisinas[1]

Received: 1 March 2022 / Accepted: 13 November 2022 / Published online: 27 November 2022

Abstract
In this work, the influence of Cr^{3+} ions on the formation of calcium silicate hydrates in the $CaO–SiO_2{\cdot}nH_2O–H_2O$ system and the thermal stability of the synthesized compounds in the temperature range of 25–1000 °C were examined. The dry mixture of CaO and $SiO_2{\cdot}nH_2O$ was mixed with a solution (0, 1 or 10 g $Cr^{3+}dm^{-3}$) to reach the liquid/solid ratio equal to 10 when the CaO/SiO_2 ratio was equal to 1.5. The hydrothermal synthesis was performed in an unstirred suspension under saturated steam at 200 °C temperature when hydrothermal curing was equal to 1 h. It was determined that Cr^{3+} ions participate in the formation of calcium silicate hydrates during hydrothermal synthesis: they intercalate into the structure of synthesized compounds and influence the sequence of the formed compounds. These changes depend on both: the pH value and the concentration of Cr^{3+} ions in the primary solution; also, after hydrothermal treatment, all Cr^{3+} intercalated into α-C_2SH, C–S–H(I) and/or C–S–H(II) structure. The formation of high basicity CSH was promoted by the decreased reactivity of amorphous SiO_2, while the intercalation of Cr^{3+} ions into the CSH structure mainly was proven by the endothermal effect at 294 °C and additional calcinations. It was found that, during the calcination at 280 °C, chromium gradually changed its degree of oxidation from + 3 to + 6, and also calcium chromate formed. It was also elucidated that α-C_2SH substituted with Cr^{3+} ions decomposed within the 400–500 °C temperature range, while wollastonite substituted with Cr^{3+} and other dibasic CSH (belite, calcium olive) started to recrystallize during solid state sintering (at 800–1000 °C) together with other chromium-containing compounds. The synthesis products were characterized by XRD, FTIR, STA, SEM–EDX and AAS.

Keywords Calcium silicate hydrates substituted with chromium ions · Thermal stability · Calcination temperature · Calcium chromate · Calcium chromium oxide

Introduction

Calcium silicate hydrates (CSH) are known to be the main component (70%) in hydrated Portland cement paste [1]. CSH can form in the nature, and it can be produced during cement hydration or in a $CaO–SiO_2–H_2O$ system under hydrothermal conditions [2]. CSH synthesized via hydrothermal treatment excels in terms of good resistance to the aggressive environment and is known for good strength properties of the after-produced binding material [3, 4]. Nowadays, CSH is used for the production of alternative cementitious materials (ACM). It is important to emphasize that, by using ACM (known as Celitement, Solidia cement, etc.), the energy consumption and CO_2 emission associated with the cement production can be reduced by up to 70%; hence, they are more economically useful and environmentally friendly: in ACM, the CaO/SiO_2 (C/S) molar ratio can be minimized from above 3 (as in ordinary Portland cement) to equal or lower than 2 (e.g., α-C_2SH, hillebrandite, wollastonite, rankinite); for ACM precursors, activation hydrothermal synthesis (150–300 °C) or calcination at 800–1200 °C is required instead of the high temperature (1450 °C) employment used for the ordinary process; ACM can be composed of raw materials which are contaminated by various wastes of technological processes and which contain such additives as heavy metal ions [5–13].

Therefore, many authors have already considered that the crystallization and properties of CSH depend on many

✉ I. Gedeike
inga.knabikaite@ktu.lt

[1] Department of Silicate Technology, Kaunas University of Technology, Radvilenu 19, 50270 Kaunas, Lithuania

components such as the C/S molar ratio of the primary mixture, the water/solid (W/S) ratio, the duration and temperature of hydrothermal synthesis, the raw materials, the natural or contaminated additives as well as some other factors [14, 15]. Moreover, additives and impurities can influence the formation of CSH, the morphological changes and the properties of the synthesized compounds as well. One of the most common natural impurities in raw materials is Al^{3+} or alkali ions [16, 17]. Baltakys et al. [18] determined that the amount of Al_2O_3 plays an important role in the formation of several compounds. In the mixtures with 2.7% Al_2O_3, only CSH intercalated with Al^{3+} ions was formed, while the higher amount of Al_2O_3 (15.4%) encouraged the formation of calcium aluminum hydrate (CAH) C_3AH_6. Other authors [19] noted that Al^{3+} ions prevented the formation of xonotlite and promoted the formation of 1.13 nm tobermorite. Furthermore, according to them, Al^{3+} ions possibly affect the shrinkage and densification of the powders during the sintering process. Also, it was determined that alkali ions can intercalate into the crystal structure of CSH and thus change its properties. For example, Na^+ positively induced the solubility of quartz in the $CaO–SiO_2–H_2O$ system, and it also strongly changed the formation and stability of the intermediate and final products in the investigated system [1]. Also, Na^+ ions are usually used in the case of an increased hydraulic activity [20].

In recent years, more attention has been paid not only to the natural impurities occurring from the starting materials, but also to various wastes which contain heavy metal ions. The influence of metal ions on the formation of CSH depends mainly on the competition of metal ions (valence, concentration and atomic radius), the pH value, the contact time and temperature [21]. Therefore, in order to understand how these specially added impurities change the formation sequence of CSH or their properties (for instance, the specific surface area, morphological structure, or the properties of conductivity), several experiments were conducted. For example, Niuniavaite et al. [22] showed that Cr^{3+}, Cu^{2+} and Co^{2+} ions can be adsorbed by synthetic C–S–H (hydrothermal synthesis at 175 °C for 16 h) whose C/S molar ratio was equal to 1.5. After Cr^{3+} ions adsorption at 25 °C for 1 h, the specific surface area of C–S–H increased up to 105.41 $m^2 \cdot g^{-1}$. Mantini et al. [23, 24] determined that Fe^{2+} can also be used for intercalation, and it is octahedrally coordinated in the phases of C–S–H (direct synthesis in MilliQ water, N_2 atmosphere, 2 weeks). The experiment indicates significantly stronger bonding of Fr^{3+} to C–S–H phases compared to Al^{3+}. Meanwhile, Chen et al. [25] removed the heavy metal ions (Pb^{2+}, Cu^{2+}, Zn^{2+} and Ni^{2+}) from wastewater by intercalation into C–S–H (reaction-rate-controlled precipitation, ambient temperature) nanosheets which later were used for photocatalytic reduction. It was determined that, after collecting Ni^{2+} ions by C–S–H, the samples became a semiconductor called nickel silicate hydroxide. Siauciunas et al. [26] found that an additive of low basicity CSH substituted with Cd^{2+} ions can be successfully used in ACM based on α-C_2SH.

However, the literature about heavy metals intercalation during the synthesis and their influence on the chemical or physical changes of the synthesized compounds is scarce. The process of the intercalation of heavy metals, especially chromium, by CSH could also be used for worldwide problems, such as solving the soil and wastewater contamination [27]. Several industrial activities (leather tanning, wood preservation, metal finishing, chromium chemical production, textile dying, pulp and paper production, etc.) are the main sources of Cr pollution [28–30]. Chromium is bioavailable and harmful, it can easily enter the food chain, and thus cause allergic, toxic, mutagenic and cancerogenic troubles in the ecosystem [31–33]. Partial studies have shown that chromium ions can be utilized from the solution by the already synthesized CSH adsorption or during CSH hydrothermal synthesis [34]. Also, they exert influence on the mineralogical composition of the formed compounds: accordingly, separate compounds (chromium hydroxide) were formed, or the crystallinity of CSH was changed (a small amount of Cr^{3+} ions additive activated α-C_2SH crystallization, while a higher amount accelerated only the formation of semicrystalline type compounds). Hopefully, the compounds synthesized under hydrothermal conditions can be used for ACM production. In this case, it is important not only to indicate the influence of Cr^{3+} ions on the formed compounds in the $CaO–SiO_2 \cdot nH_2O–H_2O$ system, but also to investigate their thermal stability: whether the main compounds, which are hydraulically active after hydrothermal treatment, can be applied in the Celitement technology, or in the Solidia cement technology, as in this case calcinated calcium silicates can be hardened without hydraulic properties. Therefore, in the first stage of the experiment, it is necessary to investigate Cr^{3+} influence on the mineralogical composition of the formed compounds when choosing the appropriate concentration of Cr^{3+} ions. And, in the second stage, it is necessary to investigate the thermal stability of the formed compounds and to present the sequence of the newly formed compounds. Due to the obtained results, it is expected that it would be possible to predict the method which is appropriate for the synthesis of the hydraulically active compounds and the ACM producing technologies. Therefore, in this article, we examined not only the influence of Cr^{3+} ions on the formation of compounds in the $CaO–SiO_2 \cdot nH_2O–H_2O$ system, but also the composition of the synthesized compounds and their thermal stability in the temperature range of 25–1000 °C.

Materials and methods

The raw materials consisted of:

- amorphous $SiO_2 \cdot nH_2O$ (Reaktiv, Russia). It was produced by grounding the delivered material for 180 s, 15 rpm speed in a vibrating cup mill Pulverisette 9 (Fritsch, Germany). Parameters: loss of ignition–6.39%, surface area–2073 $m^2\ kg^{-1}$ (Cilas ID 1090, USA).
- calcium oxide CaO (Honeywell, Germany). It was produced by calcinating $Ca(OH)_2$ at 550 °C for 1 h and grounding it for 30 s, 10 rpm speed in a vibrating cup Pulverisette 9. Parameters: the quantity of active CaO–93%, surface area–1889 $m^2\ kg^{-1}$.

The dry mixture was mixed with distilled water or $Cr(NO_3)_3 \cdot 9H_2O$ solution (Eurochemicals, EU) to reach the liquid/solid (W/S) ratio equal to 10 when the CaO/SiO_2 (C/S) ratio was equal to 1.5. The concentration of Cr^{3+} ions in the primary solution was equal to 1 or 10 g $Cr^{3+}\ dm^{-3}$ (96.15 or 288.46 Cr^{3+} mol m^{-3}).

The hydrothermal synthesis was carried out in an unstirred suspension under saturated steam at 200 °C temperature, when hydrothermal curing was equal to 1 h. After the hydrothermal treatment, the obtained products were filtered off, rinsed with acetone, dried at 80 °C ± 5 for 24 h, and sieved though a mesh (< 80 m).

The mineralogical composition of the synthesized compounds was determined by X-ray diffraction (XRD, D8 Advance diffractometer, Bruker AXS, Karlsruhe, Germany). The parameters of analysis were as follows: 0.02 mm Ni filter, Cu Kα radiation, 40 kV tube voltage, 40 mA tube current, Bruker LynxEye detector. The diffraction patterns were recorded in the Bragg–Brentano geometry within the 2θ range of 3–70° at a scanning speed of 6° min^{-1}.

Fourier transform infrared spectroscopy (FTIR) was implemented with PerkinElmer Spectrum X system (PerkinElmer, Waltham, MA, USA). Spectral analysis was carried out in the range of 4000–400 cm^{-1} with spectral resolution.

The measurements of the thermal stability and phase transformation were conducted with simultaneous thermal analysis (STA: DSC and TG). STA was carried out with the Linseis PT1000 instrument (Linseis, Selb, Germany). The parameters of analysis are given as follows: 15° min^{-1} heating rate, 30–1000 °C temperature range, nitrogen atmosphere, ceramic sample holders, Pt crucibles and ~ 10 mg mass of the sample.

The microstructure of the synthesized compounds was studied by using scanning electron microscopy (SEM) and energy-dispersive X-ray spectroscopy (EDX). SEM was performed by using a JEOL JSM-7600F instrument (Jeol, Tokyo, Japan). The operating condition was as follows: 10 kV acceleration voltage, 8.6 mm working distance, 500–50,000 times magnification. The SEM also incorporates EDX, which provides an opportunity to expand the possibilities of the analysis.

The concentration of Cr^{3+} ions was determined with a PerkinElmer Analyst 400 atomic adsorption spectrometer (AAS) (PerkinElmer, Waltham, MA, USA). The parameters of the apparatus are as follows: 357.87 nm wavelength, 30 mA current of a hollow cathode lamp, C_2H_2-air flame, 10 $dm^3\ min^{-1}$ oxidant air flow and 2.5 $dm^3 min^{-1}$ acetylene flow.

Results and discussion

Intercalation of $Cr.^{3+}$ ions into α-C_2SH and C–S–H(I) and/or C–S–H(II) structure during hydrothermal treatment (1 h, 200 °C)

It was determined that a low quantity of Cr^{3+} ions (1 g $Cr^{3+}\ dm^{-3}$) in the primary mixture ($CaO/SiO_2 = 1.5$) had a positive influence on the formation of calcium silicate hydrates because, after 1 h of hydrothermal curing at 200 °C, α-C_2SH substituted with Cr^{3+} ions (α-C_2SH–Cr) (intensity of the main α-C_2SH peak (d–0.327 nm) increased from 9.24 to 13.02 counts·s^{-1} comparing to the pure system) and semicrystalline calcium silicate hydrate C–S–H(I) and/or C–S–H(II) substituted with Cr^{3+} ions (C–S–H(I)–Cr/C–S–H(II)–Cr) were formed (Fig. 1a, curves 1 and 2). Also, in the $CaO–SiO_2 \cdot nH_2O–H_2O$ system with additive of Cr^{3+} ions, less portlandite ($Ca(OH)_2$, PDF No. 44–1481) was formed compared to the pure system (respectively, the intensity was equal to 14.63–22.03 counts·s^{-1}, while the peak area was 7.969–9.693 a.u. (d–0.491 nm, 2θ–18.05°)). It could be influenced by the pH value changes during hydrothermal treatment: it increased from 2.88 (Eq. 1) to 11.5. The lower pH value intensified the reaction of CaO at the beginning, and, later on, the compounds, which are stable in the alkaline media, were dominant in the products (Fig. 1a, curve 2).

These experiments corroborate previous results. According to the literature [35], α-C_2SH can form even at a low molar ratio (C/S < 1.25). For example, it was found that, after 4 h of isothermal curing at 200 °C temperature (C/S = 1.5), α-C_2SH, portlandite and calcite formed, while other scientists [14] found that, under similar synthesis conditions (4 h, 200 °C, C/S = 1.75), with the abovementioned compounds, C–S–H(I) and/or C–S–H(II) crystallized. Gendvilas et al. [20] synthesized α-C_2SH (4 h, 200° C) in mixtures whose molar C/S ratio was equal to 2. Therefore, it is clear that the formed compound's structure and composition in the $CaO–SiO_2 \cdot nH_2O–H_2O$ system depend not only on the molar C/S ratio, but also on some other properties, such as the temperature, stirring, hydrothermal curing time, and additives.

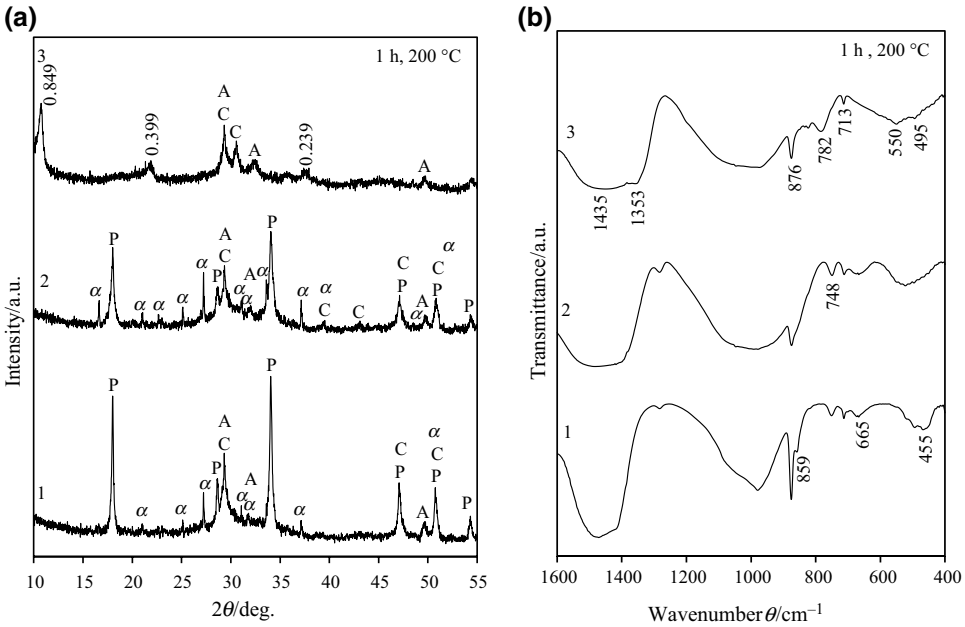

Fig. 1 XRD (**a**) and FTIR (**b**) patterns of the synthesis products, when Cr^{3+} ions concentration in primary solutions was equal, g Cr^{3+} dm^{-3}: 1–0; 2–1; 3–10. Indexes: A–pure C–S–H (I) and/or C–S–H (II) or substituted with Cr^{3+} ions; α–pure α-C_2SH or substituted with Cr^{3+} ions; C–calcite; P–portlandite

The obtained FTIR results allowed us to confirm that, due to partially unreacted amorphous SiO_2, which could be identified in the wavenumber range 1250–800 cm^{-1} (symmetrical υ_s(O–SiO–) vibrations), the C/S ratio of the synthesized compounds increased from 1.5 to 2 (Fig. 1b). Meanwhile, the formation of C–S–H(I)(–Cr) and/or C–S–H(II) (–Cr) and α-C_2SH(–Cr) was proven by the absorption band in the 700–400 cm^{-1} (δ(O–Si–O) and δ(Si–O–Si)) frequency range. Furthermore, in the system without Cr^{3+} ions additive, less intensive maximums of adsorption at 1436–876 cm^{-1} ($\upsilon(CO_3^{2-})$ and $\delta(C–O_3^{2-})$) were identified. At 800–500 cm^{-1}, the Si–O–Cr^{3+} absorption band was observed [36] (Fig. 1b, curves 2 and 3).

XRD and FTIR results were confirmed with STA (DSC, TG). Endothermal effects at the beginning (35–200 °C) demonstrated a decrease in the heat flow, which corresponds to the crystallization water loss of the synthesis products (Fig. 2). The endothermic effect at 445–461 °C temperature can be assigned to two processes (portlandite and α-C_2SH(–Cr) decomposition). It is clear that the decrement of portlandite and the increment of α-C_2SH is reflected in the STA results: while the energy of the endothermal effect went down from 104.54 (the pure system) to 83.63 (the system with Cr^{3+} additive) J g^{-1}, the mass losses increased from 1.67 to 2.98 mass%: portlandite decomposition energy is higher than α-C_2SH, therefore, it decreased in the system with Cr^{3+}, and even the mass loss was higher. The following effect (650–760 °C) was declared to represent the calcite decomposition. Finally, exothermic thermal effects showed the recrystallization of C–S–H(I)(–Cr) and C–S–H(II)(–Cr) to calcium silicate (wollastonite) at ~ 810–870 °C. Furthermore, the formation of the effects of different modifications of wollastonite shifted toward a higher temperature (from 832 to 841 °C (C–S–H (I) and from 863 to 865 °C (C–S–H (II)). Therefore, it is clearly seen that even a low quantity of Cr^{3+} ions additive in the primary mixture had a similar effect as Al^{3+} or Na^+ ions: wollastonite formation occurs at a higher temperature range [1, 37].

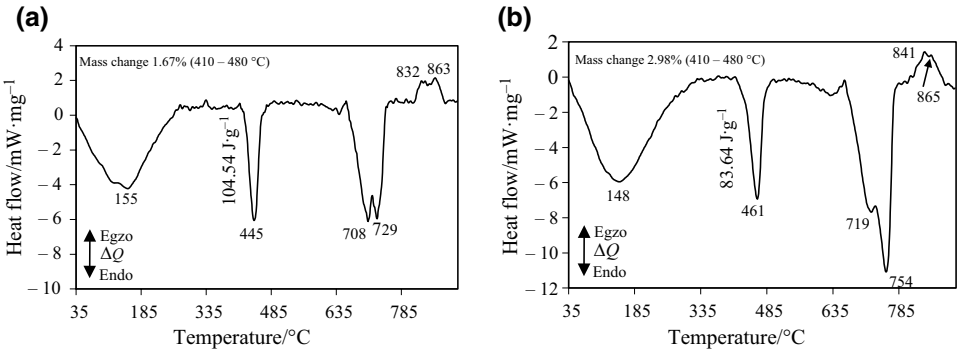

Fig. 2 DSC patterns of the synthesis products, when Cr^{3+} ions concentration in primary solutions was equal, g Cr^{3+} $dm.^{-3}$: **a** 0; **b** 1

In addition, the crystal forms and their chemical composition of the products were analyzed by SEM–EDX (Fig. 3). Due to XRD (no separate chromium-containing compounds formed), it could be supposed that Cr^{3+} ions intercalated into irregular shape α-C_2SH or close-packed particles (honeycomb) C–S–H(I) and/or C–S–H(II) structure. The additive of Cr^{3+} ions did not change the *d*-spacing values of the formed compounds; therefore, it is impossible to identify other crystalline type compounds by the XRD method. However, according to the EDX image (Fig. 3b), Cr^{3+} ions were dispersed in the whole investigation area. These data are in agreement with the AAS analysis which stated that the residual of Cr^{3+} ions in the liquid phase after hydrothermal curing was less than 0.01%.

Furthermore, it was investigated that the additive of 10 g Cr^{3+} dm^{-3} in the primary mixture negatively influenced the crystallization of the synthesis products, but positively affected the interaction with portlandite (Fig. 1a, curve 3) which is stable in a strongly basic media [38]. Meanwhile, under experimental conditions, the pH value of the liquid phase varied from 2.08 before hydrothermal treatment to 8.03 after it. According to literature [39] when the pH value is lower than 3, $Cr(NO_3)_3$ dissociates as shown in the reaction as follows:

$$2Cr(NO_3)_3 + 6H_2O \rightarrow Cr^{3+} + CrOH^{2+} + 5OH^- + 6H^+ + 6NO_3 \quad (1)$$

A higher concentration of H^+ ions caused the low values of pH before synthesis. After hydrothermal curing for 1 h, the medium became slightly alkaline, which influenced the destruction of portlandite (which is otherwise stable when pH = 11.5–14.0 [40]), and which also damaged the stability of α-C_2SH–Cr (Fig. 1, a, curve 3).

For this phenomenon, in the system, a small amount of various chromium-containing compounds could form: according to the data from the PDF-4 database, these diffraction maximums (0.849, 0.399 and 0.239 nm) could belong to these compounds which are described in Table 1.

Only agglomerates of the amorphous phase were dominated in the SEM micrographs (Fig. 4a). Furthermore, it was evidently seen that the synthesized sample consisted not only of Ca, Si, and O atoms, but also of Cr, which had been intercalated in both crystalline and amorphous structure compounds (Fig. 4b). It was proven by AAS analysis that the liquid phase did not contain Cr^{3+} ions. Therefore, these experiments are in line with the previous results [41, 42].

Table 1 The comparison of compounds *d*-spacing by date of PDF-4 database

Estimated *d*-spacing/nm		0.849	0.399	0.239
PDF No	Formula	*d*-spacing in PDF patterns/nm		
1–73–8406	CrO(OH)	–	0.409	0.241
38–292	$Ca_5Cr_3O_{12}$	0.872	0.402, 0.398	0.238
44–604	$3CaO{\cdot}Cr_2O_3{\cdot}CaCO_3{\cdot}11H_2O$	0.795	0.397	0.236

The desorption test confirmed that, during hydrothermal synthesis, chemosorption took place across the entire range of the experimental conditions (1 or 10 g Cr^{3+} dm^{-3}); the incorporation of Cr^{3+} ions in the synthesis of CSH was irreversible. In order to confirm this fact, after the hydrothermal curing, the synthesized compounds were dried and immersed in distilled water (W/S = 100), and the temperature of 25 °C was sustained for 45 min. After the experiment, AAS analysis showed that the concentration of Cr^{3+} ions did not exceed 0.01% in the liquid media.

Thermal stability of α-C_2SH-Cr and C-S–H(I)-Cr and/or C-S–H(II)-Cr compounds within 25–1000 °C temperature range

With the objective to identify the mineralogical composition and stability of the formed compounds, the samples were calcinated at 280, 500 and 1000 °C temperatures. The decomposition of the compounds containing chromium proceeded within the temperature range of 100–395 °C (Table 2) [43, 44] and two endothermic effects (at 148 and 294 °C) were identified in the DSC curve (Fig. 5).

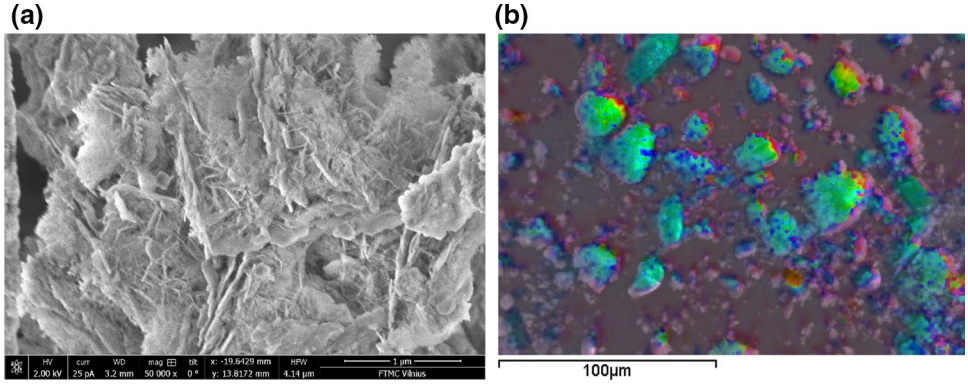

Fig. 3 SEM micrograph (×50,000) **a** and EDX images (×1500) **b** of the synthesis products, when the Cr^{3+} ions concentration in primary solutions was equal to 1 g Cr^{3+} $dm.^{-3}$. Atoms in the mapping: Ca–36.63% (light blue), Cr–0.99% (purple), Si–22.27% (green), O–40.12% (red)

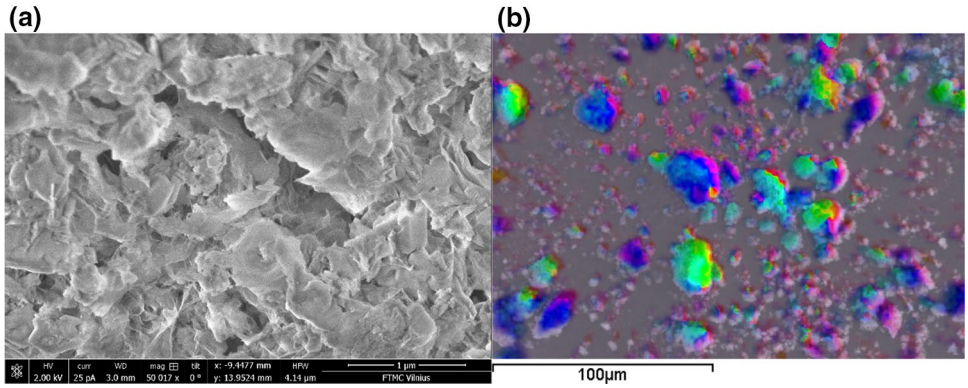

Fig. 4 SEM micrograph (×50,000) (**a**) and EDX images (×1500) (**b**) of the synthesis products, when the Cr^{3+} ions concentration in primary solutions was equal to 10 g Cr^{3+} $dm.^{-3}$. Atoms in the mapping: Ca–31.75% (light blue), Cr–8.48% (purple), Si–21.51% (green), O–38.26% (red)

Table 2 Thermal decomposition of chromium (III) nitrate (V) nonahydrate

Compound before thermal treatment	Thermal treatment temperature/ °C	Compound after thermal treatment
$Cr^{III}_{1-x}Cr^{VI}_{x}O_y(OH)_w(NO_3)_t{\cdot}pH_2O$	~100–170	$Cr^{III}_{1-x}Cr^{VI}_{x}O_y(NO_3)_t$
$Cr^{III}_{1-x}Cr^{VI}_{x}O_y(NO_3)_t$	~150–200	$Cr^{III}_{\sim 0.01}Cr^{VI}_{\sim 0.99}O_{\sim 2.99} + (NO_2, O_2)$
$Cr^{III}_{\sim 0.01}Cr^{VI}_{\sim 0.99}O_{\sim 2.99}$	~200–395	$Cr^{III}_{\sim 0.15}Cr^{VI}_{\sim 0.85}O_{\sim 2.70}$

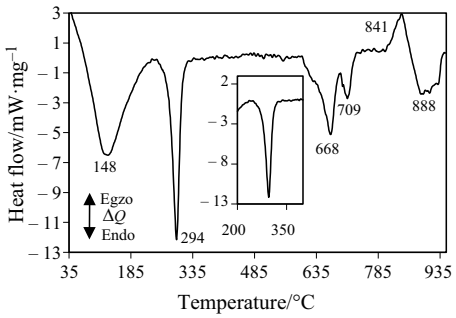

Fig. 5 DSC patterns of the synthesis products, when Cr^{3+} ions concentration in primary solutions was equal to 10 g Cr^{3+} $dm.^{-3}$

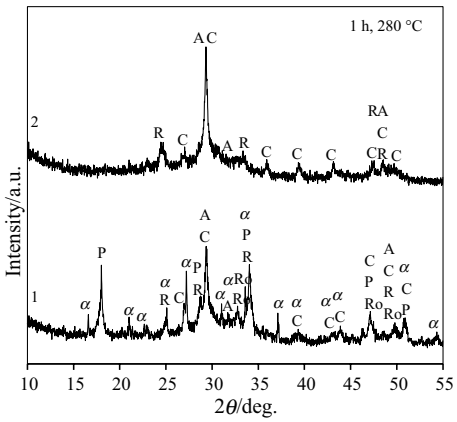

Fig. 6 XRD patterns of the calcined (1 h; 280 °C) synthesis products, when Cr^{3+} ions concentration in primary solutions was equal, g Cr^{3+} dm^{-3}: 1–1; 2–10. Indexes: A—C–S–H (I) and/or C–S–H (II) substituted with Cr^{3+} ions; α–C_2SH substituted with Cr^{3+} ions; C – calcite; P–portlandite; R–calcium chromate; Ro–calcium chromium oxide

Calcium chromate ($CaCrO_4$, PDF 1–87–1647) and calcium chromium oxide ($Ca_3Cr_3O_8$, PDF 4–21–2689) were determined to form at 280 °C, while other hydrothermal synthesis products remained stable (Fig. 6). This is consistent with the data presented in Table 2, where chromium gradually changed its oxidation degree in the range (+3)–(+6) within the 100–395 °C temperature range.

The calcination at 500 °C proved that portlandite and α-C_2SH fully recrystallized to the amorphous phase (when synthesis was performed with 1 g Cr^{3+} dm^{-3}), while calcium chromate (which formed at 280 °C) remained stable under all experimental conditions (Fig. 7). However, calcium chromium oxide became metastable and recrystallized to more stable compounds.

EDX analysis confirmed that, after calcination at 500 °C temperature, Cr^{3+} ions remained intercalated into the amorphous structure CSH or formed $CaCrO_4$ (Fig. 8 and Table 3).

Chromium-containing compounds (calcium chromium siliceous oxide and/or calcium chromium oxide ($Ca_5Cr_2SiO_{12}$, $Ca_5Cr_3O_{12}$ and/or $Ca_5Cr_3O_4$; PDF No. 38–292, PDF No. 38–293 and/or PDF No. 38–294) and uvarovite ($Ca_3Cr_2(SiO_4)_3$; PDF No. 4–7–6462)) were observed when the temperature of calcination was equal to 1000 °C (Fig. 9). Meanwhile, α-C_2SH–Cr and C–S–H(I)–Cr and/or C–S–H(II)–Cr recrystallized at a higher temperature to more stable CSH forms: wollastonite ($CaSiO_3$; PDF No. 44–11–265 and/or 4–10–2581), belite (β-Ca_2SiO_4; PDF No. 33–302) and calcium olivine (γ-Ca_2SiO_4; PDF No. 4–12–6734). Also, CaO (PDF No. 37–1497) could be

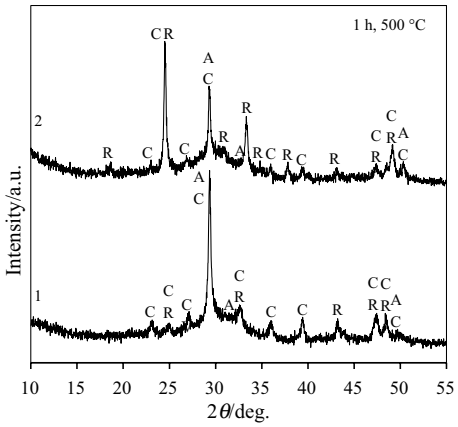

Fig. 7 XRD patterns of the calcined (1 h; 500 °C) synthesis products, when Cr^{3+} ions concentration in primary solutions was equal, $Cr^{3+}g/dm^3$: 1–1; 2–10. Indexes: C–calcite; R–calcium chromate

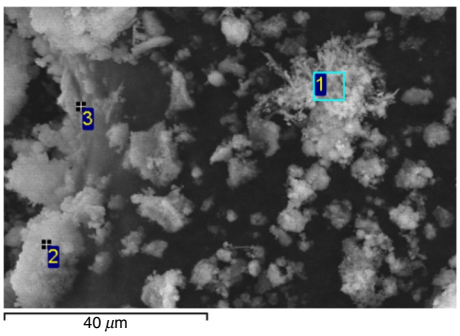

Fig. 8 SEM micrograph of calcinated (1 h, 500°) synthesis products, when the Cr^{3+} ions concentration in primary solutions was equal to 10 g Cr^{3+} $dm.^{-3}$

Table 3 EDX analysis of calcinated (1 h, 500°) synthesis products, when the Cr^{3+} ions concentration in primary solutions was equal to 10 g Cr^{3+} dm^{-3}

Spectrum No	Chemical element and Mass/%			
	Ca	Cr	Si	O
1	18.28	3.1	12.01	66.52
2	31.32	3.3	13.09	52.18
3	23.17	34.51	1.37	40.95

identified as the decomposition product of $CaCO_3$ which decomposed at 650–750 °C.

According to EDX analysis, it was clear that Cr^{3+} ions remained intercalated into more stable monobasic or dibasic CSH forms (wollastonite-Cr, belite-Cr and/or olivine-Cr) or formed separate chromium-containing oxides (see Fig. 10 and Table 4).

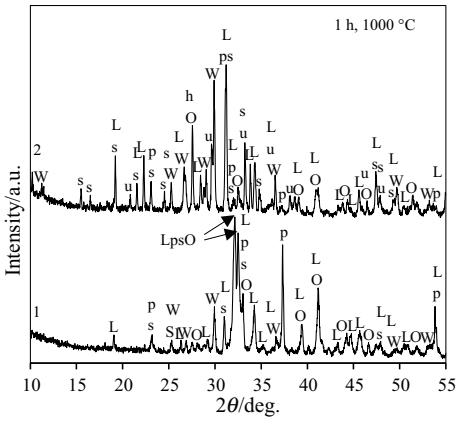

Fig. 9 XRD patterns of the calcined (1 h; 1000 °C) synthesis products, when Cr^{3+} ions concentration in primary solutions was equal, $Cr^{3+}g/dm^3$: 1–1; 2–10. Indexes: L–belite substituted with Cr^{3+} ions; O–calcium olivine substituted with Cr^{3+} ions; p–calcium oxide; s–calcium chromium silicon oxide and/or calcium chromium oxide; u–uvarovite; W–wollastonite substituted with Cr^{3+} ions

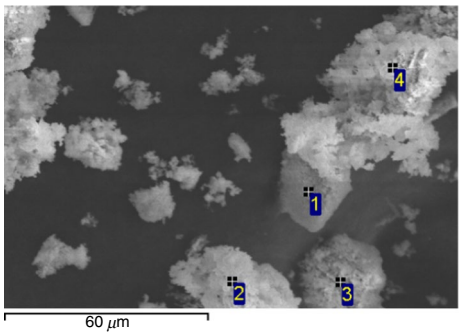

Fig. 10 SEM micrograph of calcinated (1 h, 1000°) synthesis products, when the Cr^{3+} ions concentration in primary solutions was equal to 10 g Cr^{3+} $dm.^{-3}$

Table 4 EDX analysis of calcinated (1 h, 1000 °C) synthesis products, when the Cr^{3+} ions concentration in primary solutions was equal to 10 g Cr^{3+} dm^{-3}

Spectrum No	Chemical element and Mass/%			
	Ca	Cr	Si	O
1	46.51	3.12	20.41	29.96
2	28.36	11.02	7.49	52.71
3	22.15	1.66	20.92	55.28
4	23.87	7.98	15.97	52.18

After summarizing the results, the following schematic sequence of the compounds formation in the $CaO–SiO_2{\cdot}nH_2O–H_2O$ system, and their thermal stability in the temperature range of 25–1000 °C can be proposed:

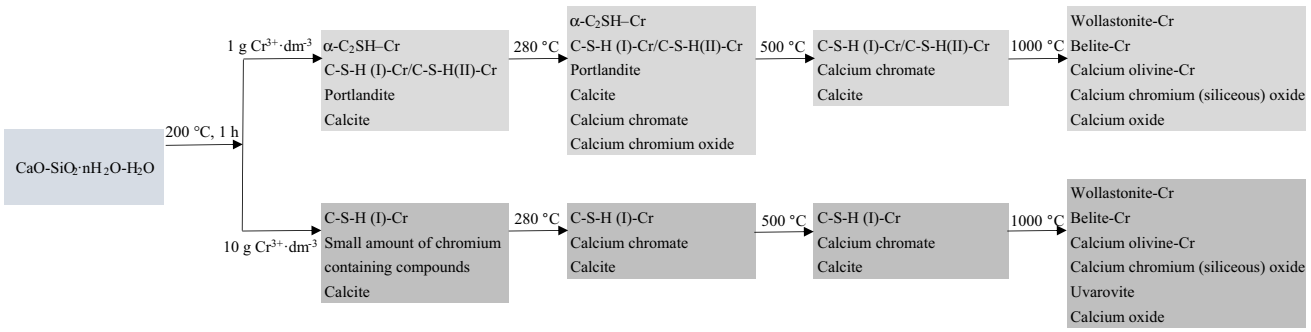

To sum up the presented results, it can be stated that chromium ions can be intercalated and utilized in the CSH structure. In other words, a technology based on these experiments could solve some environmental problems (such as soil and water contamination) as well as produce alternative binding materials (mostly α-C_2SH-Cr and wollastonite-Cr).

It was determined that 1 g Cr^{3+} dm^{-3} is the appropriate concentration for α-C_2SH–Cr synthesis, which could be used for ACM production. Therefore, in the future work, hydration experiments by already synthesized α-C_2SH–Cr would be performed. Presumably, it would be a great additive to the production of alternative binding materials. Meanwhile, C–S–H(I)–Cr/C–S–H(II)–Cr synthesized in a more concentrated system (10 g Cr^{3+} dm^{-3}) is expected to be applied for the production of adsorbents or catalysts. Yet, these assumptions still require further experimentative research.

Conclusions

It was estimated that a low concentration of chromium ions in the $CaO–SiO_2·nH_2O–H_2O$ system (C/S = 1.5) decreased the reactivity of amorphous SiO_2 and stimulated the crystallization of high basicity CSH substituted with Cr^{3+} ions: α-C_2SH–Cr, C–S–H(I)–Cr/C–S–H(II)–Cr. It should be underlined that all Cr^{3+} ions were intercalated into the structure of the formed compounds and that no other crystalline compounds containing chromium were identified.

The mineral composition of the formed synthesis products depended on both the pH value and the concentration of Cr^{3+} ions, i.e., its salt dissociation and H^+ ions quantity in the primary solution. When using a large quantity of Cr^{3+} ions (10 g Cr^{3+} dm^{-3}) additive, only semicrystalline C–S–H(I)–Cr was formed. It should be noted that the liquid phase after hydrothermal curing did not contain any Cr^{3+} ions; therefore, all Cr^{3+} ions were intercalated. However, during calcination at 280 °C temperature, the synthesized compounds became metastable, and chromium changed its degree of oxidation from + 3 to + 6; also, calcium chromate was formed. The previous compound formation was proven by DSC (endothermal effect maximum at 294 °C) and by calcination followed by XRD at 280 °C temperature.

During the solid state sintering at 800–1000 °C temperature, Cr^{3+} ions participated in the recrystallization process of crystalline compounds, which affected the formation of wollastonite-Cr which occurred at a higher temperature compared to the pure system, along with other high basicity CSH: belite-Cr and olivine-Cr, or chromium-containing compounds: calcium chromium siliceous oxide and/or calcium chromium oxide and uvarovite.

Acknowledgements This research was funded by a grant (No. S-MIP-21-256) from the Research Council of Lithuania.

Author contributions All the authors contributed to the study conception and design. The methodology and investigation plan were created by AE and KB; the material preparation, data collection and analysis were performed by IG. The first draft of the manuscript was written by IG, and all authors commented on all the intermediate versions of the manuscript. All the authors read and approved the final manuscript.

References

1. Siauciunas R, Bankauskaite A, Baltakys K, Stankeviciute M. The impact of Na2O on the synthesis of α-C2SH with different mineral composition and the stability of intermediate and final products. Ceram Int. 2018;45(2):2846–51.
2. Richardson IG. The calcium silicate hydrates. Cem Concr Res. 2008;32(2):137–58.
3. Zhang L, Yamauchi K, Li Z, Zhang X, Ma H, Ge S. Novel understanding of calcium silicate hydrate from dilute hydration. Cem Concr Res. 2017;99:95–105.
4. Foley EM, Kim JJ, Reda Taha MM. Synthesis and nano-mechanical characterization of calcium-silicate-hydrate (C-S-H) made with 1.5 CaO/SiO_2 mixture. Cem Concr Res. 2012;42(9):1225–32.
5. Gartner E, Hirao H. A review of alternative approaches to the reduction of CO_2 emissions associated with the manufacture of the binder phase in concrete. Cem Concr Res. 2015;78:126–42.
6. Stemmermann P, Schweike U, Garbev K, Beuchle G, Möller H. Celitement: a sustainable prospect for the cement industry. Cement Int. 2010;8:52–66.
7. Fang Y, Chang J. Rapid hardening β-C2S mineral and microstructure changes activated by accelerated carbonation curing. J Therm Anal Calorim. 2017;129:1–9.
8. Abd Rashid R, Shamsudin R, Abdul Hamid MA, Jalar A. Low temperature production of wollastonite from limestone and

silica sand through solid-state reaction. J Asian Ceram Soc. 2014;2:77–81.
9. Sahu S, Decristofaro N. (2013) Solidia Cement TM Part One of a Two-Part Series Exploring the Chemical Properties and Performance Results of Sustainable Solidia Cement TM and Solidia Concrete TM. Solidia Cem. 1–12
10. Ferraro G, Romei L, Fratini E, Chen SH, Jeng US, Baglioni P. Functionalised nanoclays as microstructure modifiers for calcium and magnesium silicate hydrates. Phys Chem Chem Phys R Soc Chem. 2021;23:2630–6.
11. Gartner E, Sui T. Alternative cement clinkers. Cem Concr Res. 2018;114:27–39.
12. Stemmermann P, Garbev K, Gasharova B, Beuchle G, Haist M, Divoux T. Chemo-mechanical characterization of hydrated calcium-hydrosilicates with coupled Raman- and nanoindentation measurements. Appl Geochem. 2020;118:104582.
13. Jain JA, Seth A, DeCristofaro N. Environmental impact and durability of carbonated calcium silicate concrete. Constr Mater. 2019;172:179–91.
14. Baltakys K, Dambrauskas T, Siauciunas R, Eisinas A. Formation of alpha-C_2S hydrate in the mixtures with CaO/SiO_2=1.75 by hydrothermal treatment at 200 degrees C. Rom J Mater. 2014;44:109–15.
15. Dambrauskas T, Baltakys K, Eisinas A. Formation and thermal stability of calcium silicate hydrate substituted with Al^{3+} ions in the mixtures with CaO/SiO_2 = 1.5. J Therm Anal Calorim. 2018;131:501–12.
16. Skibsted J, Andersen MD. The effect of alkali ions on the incorporation of aluminum in the calcium silicate hydrate (C–S–H) phase resulting from portland cement hydration studied by 29Si MAS NMR. J Am Ceram Soc. 2013;96:651–6.
17. Hôpital EL, Lothenbach B, Le SG, Kulik D, Scrivener K. Incorporation of aluminium in calcium-silicate-hydrates. Cem Concr Res. 2015;75:91–103.
18. Baltakys K, Eisinas A, Doneliene J, Dambrauskas T, Sarapajevaite G. The impact of Al_2O_3 amount on the synthesis of CASH samples and their influence on the early stage hydration of calcium aluminate cement. Ceram Int. 2019;45:2881–6.
19. Smalakys G, Siauciunas R. The hydrothermal synthesis of 1.13 nm tobermorite from granite sawing powder waste. Ceram-Silik. 2020;64(3):239–48.
20. Gendvilas R, Siauciunas R, Baltakys K. Quantitative thermal analysis of α-C2SH as a precursor for low-energy cements. J Therm Anal Calorim. 2015;121:155–62. https://doi.org/10.1007/s10973-015-4570-8.
21. Abollino O, Aceto M, Malandrino M, Sarzanini C, Mentasti E. Adsorption of heavy metals on Na-montmorillonite. Effect of pH and organic substances. Water Res. 2003;37:1619–27.
22. Niuniavaite D, Baltakys K, Dambrauskas T, Eisinas A. Microstructure, thermal stability, and catalytic activity of compounds formed in CaO-SiO2-Cr(NO3)3–H2O system. Nanomaterials. 2020;1–16:1299.
23. Mancini A, Wieland E, Geng G, Dahn R, Skibsted J, Wehrli B, et al. Fe (III) uptake by calcium silicate hydrates. Appl Geochem. 2020;113:104460.
24. Mancini A, Wieland E, Geng G, Lothenbach B, Wehrli B, Dähn R. Fe (II) interaction with cement phases: method development, wet chemical studies and X-ray absorption spectroscopy. J Colloid Interface Sci. 2021;588:692–704.
25. Chen L, Wang X, Chen Y, Zhuang Z, Chen F, Zhu Y. Recycling heavy metals from wastewater for photocatalytic CO_2 reduction. Chem Eng J. 2020;402:125922.
26. Siauciunas R, Baltakys K, Gendvilas R, Eisinas A. The influence of Cd-impure gyrolite on the hydration of composite binder material based on α-C2S hydrate. J Therm Anal Calorim. 2014;118:857–63.
27. Shahid M, Shamshad S, Rafiq M, Khalid S, Bibi I, Niazi NK, et al. Chromium speciation, bioavailability, uptake, toxicity and detoxification in soil-plant system: a review. Chemosphere. 2017;178:513–33.
28. Choppala G, Kunhirkrishnan A, Seshadri B, Park JH, Bush R, Bolan N. Comparative sorption of chromium species as influenced by pH, surface charge and organic matter content in contaminated soils. Geochem Explor. 2018;184:225–60.
29. Farid M, Ali S, Rizwan M, Ali Q, Saeed R, Nasir T, et al. Phytomanagement of chromium contaminated soils through sunflower under exogenously applied 5-aminolevulinic acid. Ecotoxicol Environ Saf. 2018;151:255–65.
30. Alemu A, Lemma B, Gabbiye N. Adsorption of chromium (III) from aqueous solution using vesicular basalt rock. Cogent Environ Sci Cogent. 2019;5:1–18.
31. Santos SCR, Boaventura RAR. Adsorption of cationic and anionic azo dyes on sepiolite clay: equilibrium and kinetic studies in batch mode. J Environ Chem Eng. 2016;4:1473–83.
32. R S, L S, B P. Biosorption characteristics of methylene blue and malachite green from simulated wastewater onto Carica papaya wood biosorbent. Surf Interfaces. 2018;10:197–215.
33. Piccolo A, Spaccini R, de Martino A, Scognamiglio F, di Meo V. Soil washing with solutions of humic substances from manure compost removes heavy metal contaminants as a function of humic molecular composition. Chemosphere. 2019;225:150–6.
34. Gedeike I, Baltakys K, Eisinas A. Thermal stability of synthetic high basicity calcium silicate hydrates substituted with Cr^{3+} ions. Mater Charact. 2022;193:112231.
35. Baltakys K, Dambrauskas T, Eisinas A, Siauciunas R. α-C2SH synthesis in the mixtures with CaO/SiO_2 = 1. 5 and application as a precursor for binder material. Sci Iran. 2016;23:2800–10.
36. Siauciunas R, Baltakys K, Baltusnikas A. Silikatinių medžiagų indtrumentinė analizė. 1st ed. Dastikas P, editor. Kaunas: Vitae Litera; 2007.
37. Dambrauskas T, Knabikaite I, Eisinas A, Baltakys K, Palou MT. Influence of Cr^{3+}, Co^{2+} and Cu^{2+} on the formation of calcium silicates hydrates under hydrothermal conditions at 200 °C. J Asian Ceram Soc. 2020;8(3):753–63.
38. Kutus B, Gácsi A, Pallagi A, Pálinkó I, Peintler G, Sipos P. A comprehensive study on the dominant formation of the dissolved $Ca(OH)_2(aq)$ in strongly alkaline solutions saturated by Ca(II). RSC Adv R Soc Chem. 2016;6:45231–40.
39. Bernardo GRR, Rene RMJ. Chromium (III) uptake by agro-waste biosorbents: chemical characterization, sorption–desorption studies, and mechanism. J Hazard Mater. 2009;170(2–3):845–54.
40. Windt L, Bleijerveld R, Humez N, Keulen A, Magnié M-C, Ruat P, et al. Re-visiting acceptance criteria calculations for monolithic waste landfill with reactive transport modeling: application to total dissolved salts (TDS). International solid waste conference proceedings. 2009;
41. Lu L, He Y, Xiang C, Wang F, Hu S. Distribution of heavy metal elements in chromium (III), lead-doped cement pastes. Adv Cem Res. 2018;31:1–40.
42. Baldermann A, Landler A, Mittermayr F, Letofsky-Papst I, Steindl F, Galan I, et al. Removal of heavy metals (Co, Cr, and Zn) during calcium–aluminium–silicate–hydrate and trioctahedral smectite formation. J Mater Sci. 2019;54:9331–51.
43. Malecki A, Malecka B, Gajerski R, Labus S. THERMAL DECOMPOSITION OF CHROMIUM (III) NITRATE (V) NANOHYDRATE Different chromium oxides CrO 1. 5 + y formation. J Therm Anal Calorim. 2003;72:135–44.

44. Kim J, Shin J, Paek S-M, Park DS, Kim S-J. Formation, thermal redox reaction and crystal structure of δ-CaCr2O4. J Solid State Chem. 2022;305:122669.